

## Integrating global chlorophyll data from 1890 to 2010

Daniel G. Boyce\*, Marlon Lewis, and Boris Worm

### Abstract

Understanding large-scale phytoplankton dynamics requires accurate, multi-decadal measurements of abundance and distribution. Since 1890, marine phytoplankton abundance has been assessed using a diverse range of sensors and observational platforms, and inter-calibrating these data have been challenging. Consequently, syntheses of historical phytoplankton data have been rarely attempted, and the need for accurate, long-term assessments of phytoplankton abundance and distribution is commonly acknowledged. Here, we derive quantitative indices of phytoplankton abundance from measurements of upper ocean transparency and color-calibrated with direct measurements of surface chlorophyll. The strong correlation and linear scaling of the predicted data enabled the construction of a comprehensive, globally intercalibrated chlorophyll time series from 1890 to 2010. The calibrated chlorophyll data reproduced the well-established spatial features of phytoplankton surface biomass and were strongly correlated with chlorophyll concentration derived from two independent remote sensing platforms discontinuously available since 1978. These results suggest that with careful statistical treatment it is possible to generate a globally integrated chlorophyll time series extending 120 years into the past. This database, which is available in the web appendices of this paper, may enable new insights in the areas of climate science, biogeochemical cycling, and marine ecosystem structure and functioning over the past century.

Marine phytoplankton play a key role in the functioning of the Earth's ecosystem, through their effects on climate (Charlson et al. 1987; Murtugudde et al. 2002; Wernand and van der Woerd 2010), geochemical cycling (Roemmich and McGowan 1995; Sabine et al. 2004), fisheries yield (Chassot et al. 2010; Chassot et al. 2007), and other important processes. Yet our understanding of macroecological phytoplankton dynamics is limited by the availability of accurate, large-scale, long-term measurements of abundance, particularly from the era predating the operations of satellite sensors (ocean color radiometry; available since 1978). Here, we construct a multi-decadal time-series of chlorophyll concentration, an indicator of phytoplankton biomass, by statistically integrating historical shipboard measurements from different sensors and sampling platforms.

Measurements of total chlorophyll pigment concentration

\*Corresponding author: E-mail: dboyce@dal.ca

### Acknowledgments

We are very grateful to all data providers, to J. Mills Flemming and M. Dowd for statistical advice, to T. Boyer and J. Smart for help with data extraction, and to P. Mattern, J. Mills Flemming, and M. Dowd for critical review. Funding was provided by the Natural Sciences and Engineering Research Council of Canada, the U.S. Office of Naval Research, the Canadian Foundation for Climate and Atmospheric Sciences, the National Aeronautics and Space Administration, and the Sloan Foundation.

DOI 10.4319/lom.2012.10.840

(Chl) capture first-order changes in phytoplankton carbon biomass, and despite some known variations in the Chl-to-carbon ratio (Geider 1987) are considered to be the best indicator of phytoplankton C biomass available on a global scale (Henson et al. 2010; Huot et al. 2007). Direct shipboard measurements of upper ocean Chl have been made since the early 1900s, first using spectrophotometric (Stokes 1864) and then fluorometric analyses of filtered seawater residues, and more recently through *in vivo* measurements of phytoplankton fluorescence (Jeffrey et al. 1997; Lorenzen 1966; Yentsch and Menzel 1963). Measurements of upper ocean transparency using the standardized Secchi disk have been made since 1866 (Collier et al. 1968; Tyler 1968) and have been used as a predictor of surface ocean Chl through empirically based optical equations (Falkowski and Wilson 1992; Lewis et al. 1988). Although the Secchi disk is one of the oldest and simplest oceanographic instruments, Chl concentrations derived from Secchi depth observations ( $Z_D$ ) are closely comparable to those estimated from direct *in situ* optical measurements or satellite remote sensing (Boyce et al. 2010; Lewis et al. 1988). Finally, standardized measurements of ocean color using the Forel-Ule (FU) comparator scale are available from 1890 to present (Forel 1890) and have been used as an indicator of biological activity (Wernand and van der Woerd 2010).

Modeling results indicate that a phytoplankton time series of ~40 years is necessary to separate natural variability from long-term change (Henson et al. 2010). Because the available continuous ocean color satellite record (currently 1997 to

2011) is presently too short, direct measurements of Chl, transparency, and color represent the only available data to assess multi-decadal phytoplankton dynamics. To this end, efforts have been directed toward developing methods to reliably merge different ocean color data (I.O.C.C.G. 2007), and several studies have combined historical and contemporary Chl data to produce synthetic Chl time series (Boyce et al. 2010; Gregg and Conkright 2002; Gregg et al. 2003; Raitos et al. 2005). Such approaches require a good knowledge of the accuracy, precision, and comparability of Chl measurements sampled from different observational platforms.

Here, we build and expand upon the methods developed in a previous study (Boyce et al. 2010), taking into account suggested improvements (Boyce et al. 2011; Mackas 2011; McQuatters-Gollop et al. 2011; Rykaczewski and Dunne 2011). By using a larger, more spatially and temporally comprehensive database and improved statistical methods, we predict Chl concentrations from available measurements of upper ocean transparency ( $Z_D$ ) and color (FU), available since 1890. After affirming the accuracy of the predictive methods, both directly measured and predicted Chl data were combined to create a globally integrated and inter-calibrated Chl database (see web appendices). We then examine the accuracy of the calibrated Chl data against more recent and spatially extensive remote sensing estimates of Chl.

## Materials and procedures

### Data

All data used in this analysis were extracted from publicly available databases (Table 1).

#### *In situ* measurements

Direct shipboard measurements of upper-ocean, *in situ*-derived Chl ( $Chl_I$ ,  $mg\ m^{-3}$ ) were extracted from the National Oceanographic Data Center (NODC), the Worldwide Ocean Optics Database (WOOD), and the International Council for the Exploration of the Sea Database (ICES).  $Chl_I$  measurements were made on discrete water samples collected at different depths, from vertical profiling instruments, or

continuous observations by shipboard flow-through systems.  $Chl_I$  values were derived by spectrophotometric techniques (Stokes 1864), *in vitro* and *in vivo* fluorometric techniques (Jeffrey et al. 1997; Lorenzen 1966; Yentsch and Menzel 1963), or chromatographic methods such as high-performance liquid chromatography (HPLC) or filtered samples (Mantoura and Llewellyn 1983).  $Chl_I$  measurements were derived using different instrumentation, on different platforms, and by different observers, but are collectively regarded as the most accurate Chl measurements available, and are commonly used to inter-calibrate Chl estimates from more indirect sources, such as remote sensing platforms. To allow comparability with Chl estimates from other sources, which almost exclusively estimate Chl in the uppermost layers of the oceans, only  $Chl_I$  collected in the upper 20 m were used in our analysis. All duplicated measurements were removed from the database before analysis.

#### *Transparency measurements*

Measurements of upper ocean transparency ( $Z_D$ , m) were collected with the standardized Secchi disk and were extracted from several publicly available databases.  $Z_D$  measurements are collected by lowering a white Secchi disk into the seawater and recording the depth at which the disk is no longer visible. Measurements of upper ocean transparency collected with the Secchi disk have been collected using a standardized methodology since 1866 and have been related to inherent and apparent optical properties measured by modern oceanographic instruments in the context of a “theory” of the Secchi disk (see Preisendorfer 1986). Secchi disk measurements have been used to infer changes in biological productivity and phytoplankton abundance in both freshwater and oceans (Boyce et al. 2010; Collier et al. 1968; Falkowski and Wilson 1992; Lewis et al. 1988; Tyler 1968). The linkage between observations of transparency and chlorophyll is through the dominant influence of marine phytoplankton on absorption and scattering of light in the upper ocean, similar to the basis of using ocean color radiometry in the inference of chlorophyll concentration in the upper ocean.

**Table 1.** Data sources.

Parameter	Symbol	Source	n Extracted	n Final	Temporal	Web site
Chlorophyll	$Chl_I$	WOOD	1,665,895	5,315	1900-2003	www.wood.jhuapl.edu/wood/
Chlorophyll	$Chl_I$	NODC	2,524,096	155,493	1933-2010	www.nodc.noaa.gov/
Chlorophyll	$Chl_I$	ICES	349,308	20,532	1934-2010	www.ices.dk/indexfla.asp
Chlorophyll	$Chl_{CZCS}$	NASA (CZCS)	NA	NA	1978-1986	oceandata.sci.gsfc.nasa.gov
Chlorophyll	$Chl_{SWFS}$	NASA (SeaWiFS)	NA	NA	1997-2011	oceandata.sci.gsfc.nasa.gov
Transparency	$Z_D$	WOOD	41,388	22,266	1903-2008	www.wood.jhuapl.edu/wood/
Transparency	$Z_D$	NODC	160,383	128,988	1899-2007	www.nodc.noaa.gov/
Transparency	$Z_D$	ICES	38,385	17,432	1903-1998	www.ices.dk/indexfla.asp
Transparency	$Z_D$	MIRC	121,436	101,053	1923-1998	www.mirc.jha.jp/en/outline.html
Transparency	$Z_D$	BIDA	8,389	304	1890-1898	links.baruch.sc.edu/
Color	FU	NODC	203,763	193,533	1890-2008	www.nodc.noaa.gov/

### **Ocean color measurements**

Measurements of upper ocean color have been recorded since 1890 using the Forel-Ule color index scale (FU). The FU observations have been collected using a standardized methodology designed to quantitatively assess the color of the upper ocean against a scale of 21 discrete colors ranging from dark blue (FU = 1) through different shades of green to brown (FU = 21); (Forel 1890). FU measurements are derived by subjectively matching the color of the seawater to that of the Forel-Ule color scale. Although the optical characteristics of the Forel-Ule measurements are largely unresolved, they have been useful in inferring long-term changes in biological activity (see recent review by Wernand and van der Woerd 2010), and may be useful in deriving upper ocean chlorophyll concentrations.

### **Radiometry measurements**

Measurements of Chl derived from remotely sensed ocean-leaving radiances were extracted from the National Aeronautics and Space Administration's (NASA) ocean color database. Chl measurements derived from the Coastal Zone Color Scanner (CZCS;  $\text{Chl}_{\text{CZCS}}$ ; 1978-1986; Hovis et al. 1980), and the Sea-viewing Wide Field-of-view Sensor (SeaWiFS;  $\text{Chl}_{\text{SWFS}}$ ; 1997-2010; McClain et al. 2004) were used. Remote sensing Chl data were extracted as monthly 9 km<sup>2</sup> resolution reprocessed Chl measurements and were spatially interpolated to 1° × 1° cells for each year and month using nearest neighbor algorithms.

### **Analysis**

The steps in this analysis included the following:

1. Quality control:  $\text{Chl}_l$ ,  $Z_D$  and FU measurements are adjusted or eliminated from the database based on objective quality-control procedures.
2. Corrections and standardizations:  $\text{Chl}_l$ ,  $Z_D$ , and FU measurements are objectively standardized to common spatial and temporal resolutions.
3. Calibration: Chl fields are predicted from  $Z_D$  and FU based on available spatial and temporal matchups with  $\text{Chl}_l$  measurements.
4. Validation: The precision and accuracy of calibrated Chl measurements are compared against independent Chl measurements to assess their accuracy.

### **Quality control: $Z_D$ and FU measurements**

To eliminate the optically confounding effects of suspended particles and dissolved organic material associated with terrigenous sources, all near-shore (<20 m water depth or <1 km from the nearest coastline)  $Z_D$  and FU measurements were removed from the database. If the time or location of the  $Z_D$  or FU measurements were erroneous, those measurements were also removed. All FU measurements less than one or greater than 21, and all  $Z_D$  measurements less than zero or greater than 60 m were treated as biologically implausible and removed from the database.

### **Quality control: $\text{Chl}_l$ measurements**

The  $\text{Chl}_l$  measurements used here have been collected since 1900 by different institutions and methods, and their accu-

racy may be affected by weather conditions, incorrectly calibrated instrumentation, sampling technique, data digitization errors, the optical complexity of seawater, and other factors. Due to the central importance of the  $\text{Chl}_l$  measurements to the subsequent calibration exercise and the larger number of factors potentially affecting their accuracy, the  $\text{Chl}_l$  measurements were rigorously filtered to remove any erroneous measurements. As for FU and  $Z_D$  measurements, all near-shore  $\text{Chl}_l$  measurements (<20 m depth or <1 km from the nearest coastline) and those with erroneous locations and time were removed.  $\text{Chl}_l$  measurements were identified as statistical outliers if they i) were greater than 75 mg m<sup>-3</sup>; ii) were below the published limit of detection (0.01 mg m<sup>-3</sup>; Wiltshire et al. 1998); or iii) were identified as outliers by NODC quality control methods (details in Conkright et al. 2002). Our analysis revealed that a small fraction of the  $\text{Chl}_l$  database contained outlying values, which were likely uncalibrated fluorescence measurements (Boyer et al. 2009). Such errors are likely systematically dependent on the cast, cruise, or observer associated with the outlying  $\text{Chl}_l$  measurement. To account for this,  $\text{Chl}_l$  measurements collected in casts or cruises where over 10% of all measurements were flagged as outliers by the previous criteria were removed from the database. Whereas some erroneous measurements will remain, these represent a small fraction of the entire  $\text{Chl}_l$  database and constitute a random, rather than systematic departure from the mean. Following this step, all remaining outlying individual  $\text{Chl}_l$  measurements in the database were removed.

$\text{Chl}$  measurements of 0 mg m<sup>-3</sup> accounted for a small fraction (~0.4%) of all  $\text{Chl}_l$  data but are biologically implausible in even the most oligotrophic marine waters. These measurements may either reflect data collection or digitization errors or valid measurements, which are below the detection limit of the sampling instrument. To identify and remove erroneous zero- $\text{Chl}$  values and to estimate the true but unknown zero- $\text{Chl}$  values, we fit an objective function relating  $\text{Chl}$  to sampling depth for each cast according to the number of  $\text{Chl}_l$  measurements in each cast:

For casts containing more than six unique  $\text{Chl}_l$  measurements, zero- $\text{Chl}_l$  values were assessed based on an empirically based function relating  $\text{Chl}_l$  to the sampling depth. Zero  $\text{Chl}_l$  values falling within the 95% confidence levels of the fitted function were assumed to be true data, which were below the limit of detection and were readjusted to 50% of the minimum  $\text{Chl}$  value within the cast. If this adjusted value was greater than the lowest limit of detection (0.01 mg m<sup>-3</sup>) then the values were again readjusted to 0.005 mg m<sup>-3</sup>. Zero  $\text{Chl}_l$  values falling outside the confidence limits of the function were identified as erroneous and removed from the database.

For casts containing between one and six additional measurements, if the lowest recorded  $\text{Chl}_l$  value was greater than 0.01 mg m<sup>-3</sup> then the zero- $\text{Chl}_l$  value was assumed to be erroneous and was removed from the database. Otherwise, the zero  $\text{Chl}_l$  values were adjusted to 50% of the minimum  $\text{Chl}_l$

value in the cast. If this adjusted value was greater than 0.01 mg m<sup>-3</sup> then the values were again readjusted to 0.005 mg m<sup>-3</sup>.

These corrective algorithms were visually inspected for each cast to ensure adequate performance. All zero-Chl<sub>l</sub> measurements contained within casts with less than two additional measurements were eliminated from the database.

Even within the upper 20 m of the water column, Chl<sub>l</sub> values can vary over several orders of magnitude, in part due to nonphotochemical quenching of fluorescence. To account for this variability, mean Chl<sub>l</sub> measurements were calculated over depth for each cast under an assumption of a well-mixed surface layer. Alternate depth interpolations such as the depth-weighted mean, median, Akima method (Akima 1978), wavelets, polynomials, and generalized additive models (Hastie and Tibshirani 1986; Wood 2006) relating Chl<sub>l</sub> to the sampling depth were used but did not improve the results.

Global spatial patterns of chlorophyll at intra-annual timescales vary in a distinct and well-established manner (Doney et al. 2003; Mahadevan and Campbell 2002). Spatial filters were used to identify extreme outlying Chl<sub>l</sub> measurements. For each annual season ( $n = 4$ ), a flexible spatial trend surface was fitted to the Chl<sub>l</sub> data. This was accomplished by fitting an additive model (Wood 2006) to the data as follows:

$$\ln(\mu_i) = B_0 + f_i(\text{Latitude}_i, \text{Longitude}_i) + \epsilon_i \quad (1)$$

where  $\ln(\mu_i)$  is the expected mean log-transformed Chl<sub>l</sub> concentration,  $B_0$  is the model intercept,  $f_i$  is the nonparametric effect estimated from the data, and  $\epsilon_i$  is an error term. Measurements, which were more than 12 standard deviations from the fitted spatial surface, were flagged as extreme outliers and removed from the database ( $n = 930$ ). This technique is comparable to the Boolean ‘range checking’ methods, which are a common quality control method for oceanographic data (Conkright et al. 2002).

Throughout these analyses, Chl<sub>l</sub> collected using ‘underway’ methods (undulating ocean recorder or towed CTD) displayed atypical frequency distributions and many statistically outlying observations. Because the accuracy of these data could not be empirically verified, they were removed from the analysis.

#### Standardizations

To examine the relationship between Chl<sub>l</sub>,  $Z_D$ , and FU data, all measurements were binned to a common spatial and temporal resolution. To balance the fine resolution necessary to accurately capture small-scale spatial variations against the coarse resolution required to obtain representative sample sizes, data were individually binned into 1° × 1° cells. Mean values per year and month for each cell ( $\text{Data}_{M,jkl}$ ) were calculated:

$$\text{Data}_{M,jkl} = \sum \text{Data}_{i,jkl} / \sum N_{i,jkl} \quad (2)$$

where  $\text{Data}_{i,jkl}$  is the data value and  $N_{i,jkl}$  is the number of measurements for cell  $j$ , month  $k$ , and year  $L$ . Objectively weighted

binning algorithms were also implemented (Boyce et al. 2010; Levy and Brown 1986; Lewis et al. 1988), but did not change the resulting parameter values within three decimal points. Hence, we used the simpler unweighted binning procedure here.

#### Calibration

Previous Chl calibration algorithms have used a linear relationship on a logarithmic scale between Secchi depth and Chl<sub>l</sub> provided that measurements are made in optically noncomplex case I waters (Falkowski and Wilson 1992; Lewis et al. 1988). The basis for this relationship is best explained through the equation relating  $Z_D$  to the optical properties of marine waters which to first order:

$$Z_D \propto 1/(c + K) \quad (3)$$

where  $c$  is the average (photopic) beam attenuation coefficient (m<sup>-1</sup>), and  $K$  is the average (photopic) diffuse attenuation coefficient (m<sup>-1</sup>), and the proportionality depends weakly on illumination, contrast of the disk and water, and visual acuity (Falkowski and Wilson 1992; Preisendorfer 1986). Variations in  $c + K$  explains the majority of the variability in transparency depths and co-varies with the amount of attenuating material in the water through its influence on the inherent optical properties such as scattering and absorption. For case I ocean waters, phytoplankton cells and co-varying biogenic dissolved matter are the principal sources of variation in the optical properties and empirically based algorithms have consequently been used to derive accurate upper ocean chlorophyll concentrations (Chl<sub>l</sub>) from transparency measurements (Boyce et al. 2010; Falkowski and Wilson 1992; Lewis et al. 1988). The nonlinear nature of the relationship reflects changes in the average size of phytoplankton cells, where rich coastal waters have a larger percentage of large cells relative to low chlorophyll waters where small cells dominate.

Forel-Ule ocean color data are positively correlated with both the transparency and chlorophyll concentration of the upper ocean but have not yet been used to derive quantitative measurements of Chl. Before attempting to calibrate these data, we examined them along with the  $Z_D$  data to establish relationships between  $Z_D$  or FU measurements and Chl<sub>l</sub> measurements.

To derive Chl values from  $Z_D$  or FU, model II ranged major axis (RMA) linear regression models were fitted to the (1° × 1° × month × year) binned data (Legendre and Legendre 1998; Sokal and Rohlf 1995). Model II RMA regression methods are appropriate when both variables in the regression equation are subject to error (Ripley and Thompson 1987), are expressed in different units, or the error variances differ (Legendre and Legendre 1998). This technique accounts for the fact that Chl<sub>l</sub>,  $Z_D$ , and FU measurements were all measured with some error and that these errors were probably unequal. Chl<sub>l</sub>,  $Z_D$ , and FU measurements were log-transformed to achieve bivariate normality, and homoscedasticity and linearity were confirmed, as required by the regression analysis. The

regression parameters from these models were estimated to predict individual Chl values from each discrete quality-controlled FU and  $Z_D$  value. Error statistics for the estimated model parameters were generated using randomized permutation tests with 1000 replicates (Legendre and Legendre 1998). The suitability of alternate models and transformations were explored, but model fit statistics indicated that they did not fit the data as well as the linear RMA models. The resulting calibrated data are denoted as  $Chl_T$  and  $Chl_F$ , derived from Secchi depths and Forel-Ule indices, respectively.

### Validation

To explore the accuracy and linear scaling of Chl measurements derived from different methods, two separate validation analyses were undertaken. The first analysis compared the accuracy of calibrated  $Chl_T$  and  $Chl_F$  measurements against each other and against the direct  $Chl_I$  measurements (three comparisons). The second analysis compared the resulting integrated calibrated Chl measurements ( $Chl_C$ ) against remotely sensed  $Chl_{SWFS}$  and  $Chl_{CZCS}$  measurements (three comparisons). Both validation analyses employed the same statistical methods and are described below.

Chl measurements derived using different observational platforms were individually objectively binned (Eq. 2) and matched spatially (1° cell) and temporally (month and year) to the Chl dataset under comparison. RMA regression models were then fitted to the log-transformed Chl matchups to examine the linear relationship between them. We used RMA as opposed to alternate model II regression techniques because it was the method used to derive  $Chl_T$  and  $Chl_F$  values, and the statistical assumptions remain valid. A Pearson correlation coefficient of 1, an estimated slope of 1, and an intercept of 0 would indicate that the Chl values from the two data sources were identical. The bias of the estimated correlation coefficients and slopes was calculated using a bootstrapping procedure with 1000 replicates (Legendre and Legendre 1998). The difference between the estimated parameter and the mean of the bootstrapped estimates provides an estimate of the bias. To further examine patterns of similarity, the standardized Euclidean residuals from RMA regression fits were calculated. These values correspond to the average difference between the two variables under comparison while minimizing the confounding effects of spatial and temporal variation. These differences were initially explored by visually inspecting the spatial distribution of the mean and absolute mean Euclidean residuals, here defined as the shortest distance between the residual and the fitted regression line. To further explore factors that may explain any systematic differences between the variables, spatially explicit univariate and multivariate linear models were fit to the residuals. Temporal (year, month), spatial (distance from the nearest coast, bathymetry, latitude, Chl), and optical (climatological CDOM index; Acker and Lepoukh 2007; Morel and Gentili 2009; Siegel et al. 2005) factors were included as possible explanatory variables. An autocovariate was included within the models to account for any

potential spatial dependence in the residuals. The autocovariate for each geographic cell ( $A_q$ ) was calculated as the weighted average of the measurements within a prespecified geographical radius of 8 nearest neighbors as

$$A_q = \sum w_{qr} y_r / \sum w_{qr} \quad (4)$$

where  $y_r$  is the measurement of  $y$  at location  $r$  among location  $q$ 's set of  $k_q$  neighbours;  $w_{qr}$  is the weight given to location  $r$ 's influence over location  $q$  (Augustin et al. 1996; Dormann 2007; Gumpertz et al. 1997). Individual weights for the autocovariate were derived as

$$w_{qr} = 1/h_{qr} \quad (5)$$

where  $w_{qr}$  is the weight given to cell  $r$ 's influence over cell  $q$ , and  $h_{qr}$  is the Euclidean distance between cells  $q$  and  $r$  (Augustin et al. 1996).

Sensitivity analyses were undertaken to determine how robust the results of these comparisons were to variation in the initial conditions of the model. The sensitivity of the estimated slopes and correlation coefficients to changing sample sizes was estimated by bootstrapping estimates (1000 replicates) at each of 18 sample sizes ranging from 10% to 100% of available matchups. Additionally, the sensitivity of the estimates to the ocean basin, bathymetry, month, and decade when the measurements were collected was also examined.

### Assessment

After removing erroneous or biologically implausible measurements and those collected in nearshore waters,  $Chl_I$ ,  $Z_D$ , and FU measurements were distributed most densely in northern temperate waters (>30°N) and closer to shore (Fig. 1A, D, G).  $Chl_I$  measurements were most abundant in the North Atlantic, whereas  $Z_D$  and FU measurements were concentrated in the North Pacific. Spatial patterns of  $Chl_I$  measurements were similar to those of  $Z_D$  and FU measurements (Fig. 1B, E, H), however the oligotrophic gyres were less clearly delineated by the relatively sparser FU measurements (Fig. 1H).  $Chl_I$  measurements were sampled since 1900, but were less available before 1955. The  $Z_D$  and FU measurements extended back to 1890 (Fig. 1C, F, I), but were less available since the 1990s. The data density for all series was greater in Northern Hemisphere summer months and since 1950.

Regression analysis revealed that the relationship between available  $Chl_I$  and  $Z_D$  matchups ( $n = 12,841$ ) was linear (log-transformed) for  $Z_D > 6$  m (Fig. 2A).  $Z_D$  measurements less than 6 m are rare in open ocean waters and are likely erroneous or associated with coastal waters with complex optical properties. Examination of available  $Z_D$ ,  $Chl_I$ , and FU matchups ( $n = 6710$ ) confirmed that most  $Z_D$  values less than 6 m corresponded to FU values greater than 10 (Fig. 2C), indicative of optically complex green or brown waters located close to coastlines (Fig. 2E). In fact, 86% of  $Z_D$  values under 6 m were located on continen-

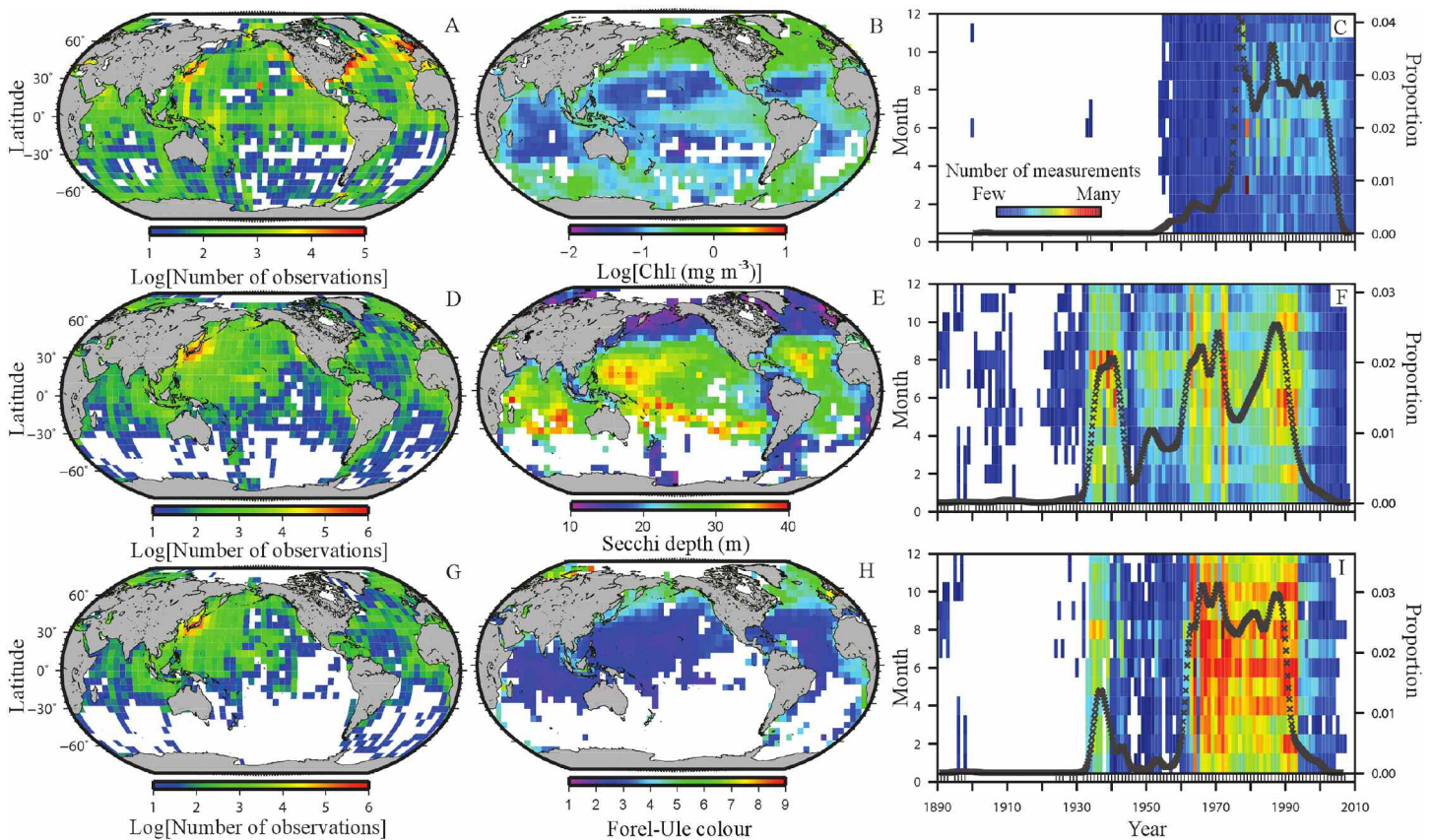


**Fig. 1.** Temporal and spatial availability of data. (A, D, G) Spatial availability of (A) Chl<sub>f</sub>, (D) Z<sub>D</sub>, and (G) FU color measurements. Colors depict the number of available measurements per 5° cell. (B, E, H) Average (B) Chl<sub>f</sub>, (E) Z<sub>D</sub>, and (H) FU color per 5° cell. Values were derived using B-spline interpolation; white indicates lack of data. (C, F, I) Time-varying availability of (C) Chl<sub>f</sub>, (F) Z<sub>D</sub>, and (I) FU measurements. Left axis and colors depict the number of available measurements by month and year. Right axis and points depict the proportion of total observations collected in each year, smoothed with kernel density. Ticks on x-axes represent years containing data.

tal shelves (<200 m depth). To eliminate Z<sub>D</sub> measurements in optically complex waters and to ensure a linear relationship between available log-transformed Chl<sub>f</sub> matchups, all Z<sub>D</sub> measurements less than 6 m were removed from the final database product (*n* = 20,748; 7% of Z<sub>D</sub> measurements).

Likewise it was determined that the relationship between available log-transformed Chl<sub>f</sub> and FU matchups (*n* = 6943) was linear for FU values between 2 and 10 (Fig. 2B). FU measurements greater than 10 corresponded to yellow and brown waters. Examination of available FU, Chl<sub>f</sub>, and Z<sub>D</sub> matchups confirmed that most FU values above 10 corresponded to extremely low Z<sub>D</sub> depths (Fig. 2D), again indicative of optically complex waters located closer to coastlines (Fig. 2E), which can confound Chl derivation techniques. In fact, 78% of FU values over 10 were located on continental shelves (<200 m depth). In contrast, FU measurements below 2 corresponded to indigo blue waters that contain the lowest Chl concentrations. The FU technique is likely unreliable in resolving subtle variations in Chl at these very low phytoplankton concentrations, as the primary determinant of ocean color is the absorption and scattering associated with pure seawater. Although

these waters may appear uniformly dark blue on the FU scale, Chl concentrations may vary over an order of magnitude or more, resulting in large variability at these FU values (Fig. 2A). To eliminate FU measurements associated with optically complex waters and to ensure a linear relationship between available Chl<sub>f</sub> matchups, FU values greater than 10 or less than 2 were removed from the final database (*n* = 10,123; 5% of all FU measurements). The removal of these FU and Z<sub>D</sub> measurements was necessary to ensure that the requisite statistical assumptions of the predictive models were satisfied.

The RMA regression was then used to predict Chl<sub>f</sub>. The regression explained 64% (*P* < 0.0001) of the variance in Chl<sub>f</sub> (Fig. 3A) and resulted in

$$\text{Chl}_f = 143.29Z_D^{-2.082} \tag{6}$$

where Chl<sub>f</sub> is the transparency-derived Chl (mg m<sup>-3</sup>). Likewise, the RMA regression used to derive Chl<sub>f</sub> explained 46% (*P* < 0.0001) of the variance in Chl<sub>f</sub> (Fig. 3B) and resulted in

$$\text{Chl}_f = 0.016\text{FU}^{2.44} \tag{7}$$

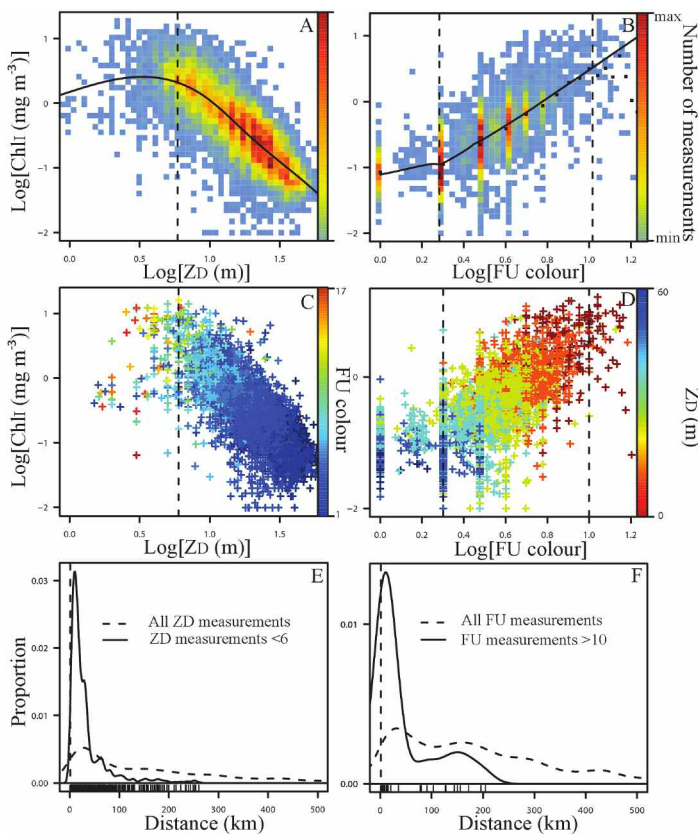


**Fig. 2.** Comparing different data types. Relationship between (A)  $Z_D$  and (B) FU and  $Chl_f$ . Relationships are approximated by a B-spline (knots = 4). Vertical dashed lines represent the thresholds, beyond which the linear relationships break down. (C-D) Colors denote the number of measurements per pixel. Relationships between  $Z_D$ , FU, and  $Chl_f$ . (C)  $Z_D$  is plotted against  $Chl_f$  with corresponding FU values indicated as colors. (D) FU is plotted against  $Chl_f$  with corresponding  $Z_D$  values indicated as colors. Dashed lines represent thresholds, beyond which the linear relationships deteriorate. (E-F) Sampling effort of (E)  $Z_D$  and (F) FU measurements as a function of distance from the nearest coastline. Solid lines indicate all available data, and dashed lines are the data that are eliminated from the database. Ticks on x-axes are the depths where the eliminated data are sampled; dashed vertical lines indicate a distance of 1 km from the nearest coastline.

where  $Chl_f$  is the FU-derived  $Chl$  ( $mg\ m^{-3}$ ). All RMA regressions conformed to the necessary statistical assumptions, such as linearity, normality, constancy of variance, and independence. Examination of the absolute Euclidean residuals from the RMA regressions indicated that the discrepancies between the predicted  $Chl$  fields ( $Chl_T$  or  $Chl_F$ ) and  $Chl_I$  were random, and could not be explained by any of the explanatory variables.  $Chl_I$  matchups used to predict  $Chl_T$  or  $Chl_F$  values were available globally, but were more heavily distributed in the northern hemisphere, and in near shore waters for both  $Z_D$  (Fig. 3C), and FU (Fig. 3D).  $Chl_I$  and FU matchups were notably lacking in open ocean waters (Fig. 3D).  $Chl_I$  matchups were slightly less available in boreal winter months for both datasets (Fig. 3E, 3F).

$Chl_T$  and  $Chl_F$  are by definition intercalibrated with  $Chl_I$  (slope = 1, intercept = 0; Fig. 4). The accuracy of these inter-

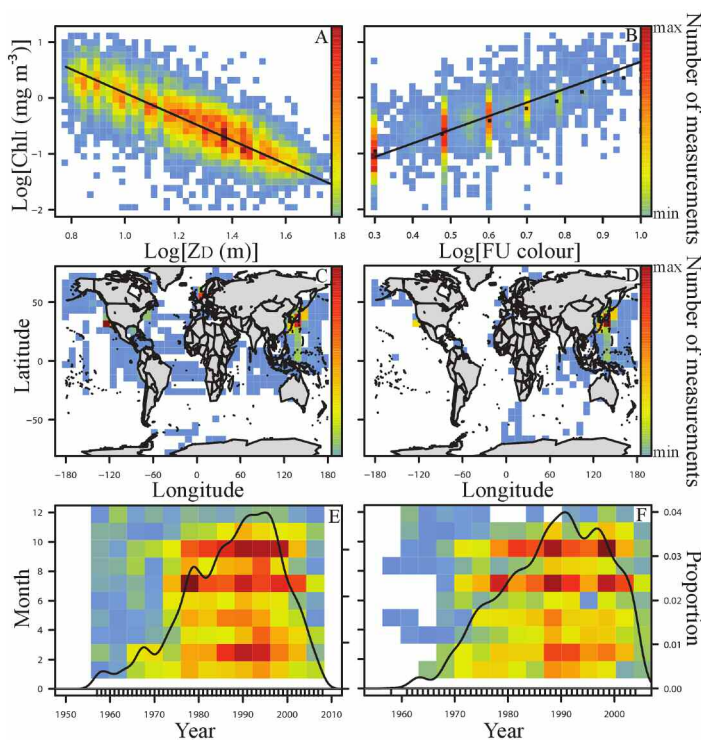


**Fig. 3.** Predicting chlorophyll from transparency and color data. Linear RMA regression models used to derive  $Chl$  from (A)  $Z_D$  and (B) FU. Confidence intervals are too narrow to visually detect. Spatial availability of  $Chl_I$  and (C)  $Z_D$ , and (D) FU matchups. Time-varying availability of  $Chl_I$  and (E)  $Z_D$  and (F) FU matchups. Left axes and colors depict the number of available measurements by month. Right axes and lines depict the proportion of total available measurements for each year. For all plots, colors depict the number of available observations per pixel.

calibrations was further verified by the strong positive correlation ( $r = 0.70$ ;  $P < 0.0001$ ) and linear scaling observed between log-transformed  $Chl_T$  and  $Chl_I$  (intercept = 0.002, slope =  $1.07 \pm 0.01$ ,  $r^2 = 0.48$ ). These calibrations were found to be insensitive to the number of measurements used, except at extremely low sample sizes. The strength of the linear relationships did not change with decreasing sample size, nor did they appreciably change with changes in the bathymetry, ocean basin, month, or decade when the measurements were collected. The magnitude of the estimated slopes varied randomly, rather than systematically. These results suggest that no further intercalibration was required before combining historical  $Chl_I$  measurements with those predicted from  $Z_D$  or FU.

The resulting calibrated database ( $Chl_C$ ) consisted of 644,916 globally distributed  $Chl$  measurements collected between 1890 and 2010. Similar to the individual  $Chl$  datasets, the sampling effort of  $Chl_C$  was heavily distributed over boreal summer months, and in more recent decades (>1930; Fig. 5A). Despite the greatly increased spatial availability of  $Chl_C$  measurements, the sampling effort remained concentrated in the northern hemisphere (>30° S latitude), over mid- to low-latitude regions, and in waters closer to

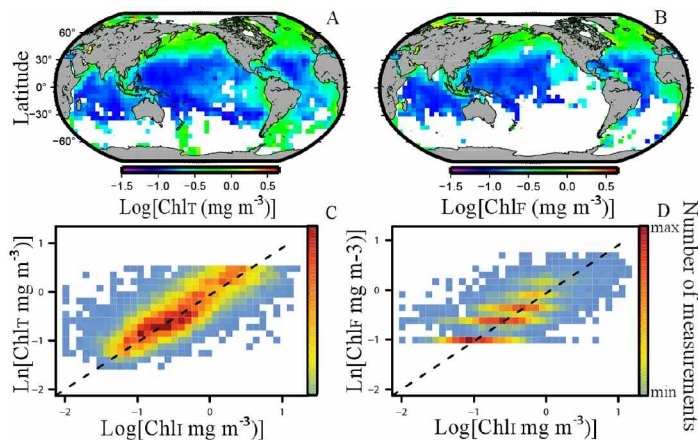


**Fig. 4.** Spatial patterns of derived chlorophyll. Mean Chl concentration from (A)  $Chl_T$  and (B)  $Chl_C$  per  $5^\circ$  cell. Relationships between available  $Chl_C$  matchups and (C)  $Chl_T$  and (D)  $Chl_{SWFS}$ . Idealized relationships are plotted as dashed lines and are identical to fitted RMA regression lines. Colors depict the number of observations per pixel.

coastlines (Fig. 5B). The  $Chl_C$  measurements are available since the 1950s in most ocean regions and before 1930 in many North Atlantic and Pacific waters (Fig. 5C). The data span more than 50 years in most regions of the ocean and 112 years in some regions of the North Atlantic. Importantly, the spatial and temporal availability of the  $Chl_C$  measurements is considerably increased after combining available historical data.

Spatial patterns of  $Chl_C$  closely reproduced the well-known spatial patterns of Chl derived from  $Chl_{CZCS}$  and  $Chl_{SWFS}$  (Fig. 6); these include elevated chlorophyll in coastal, high-latitude, and upwelling regions, as well as low chlorophyll in the oligotrophic gyres. Although there are potential issues regarding the intercalibration of  $Chl_{CZCS}$  (Antoine et al. 2005; Gregg and Conkright 2001), the  $Chl_C$  fields were positively correlated with concurrent ( $1^\circ \times 1^\circ \times 1$  month bins)  $Chl_{CZCS}$  ( $r = 0.76, P < 0.0001$ ), and exhibited approximate linear scaling on a log-scale (intercept =  $-0.01$ , slope =  $0.84, r^2 = 0.58$ ; Fig. 6C; Table 2). Likewise,  $Chl_C$  measurements were positively correlated with  $Chl_{SWFS}$  ( $r = 0.81, P < 0.0001$ ), and exhibited approx-

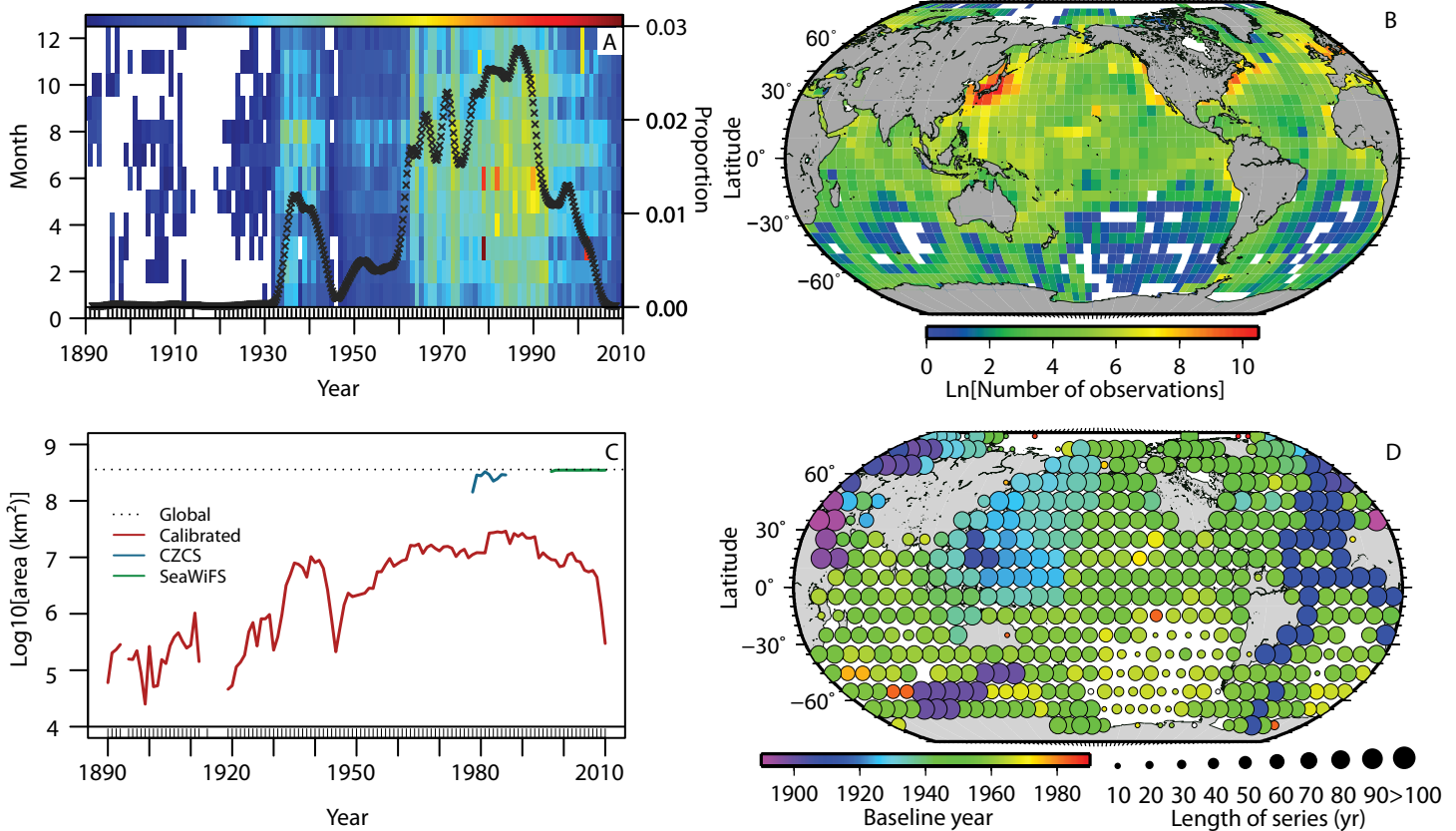


**Fig. 5.** Availability of integrated chlorophyll measurements. (A) Time-varying availability of  $Chl_C$  measurements. Left axis and colors depict the number of available measurements by month and year. Right axis and points depict the proportion of total observations collected in each year, smoothed with kernel density. Ticks on x-axis represent years containing data. (B) Spatial availability of  $Chl_C$  data. Colors depict the number of available measurements per  $5^\circ$  cell. (C) Spatial availability of  $Chl_C$ ,  $Chl_{SWFS}$ , and  $Chl_{CZCS}$  measurements through time. Colors depict the observational platform; dashed line indicates the maximum available ocean area. Tick marks on x-axis represent years containing  $Chl_C$  data. (D) Spatio-temporal availability of  $Chl_C$  measurements. Colors depict the baseline year, size of the circles depicts the temporal span of available data per  $10^\circ$  cell.

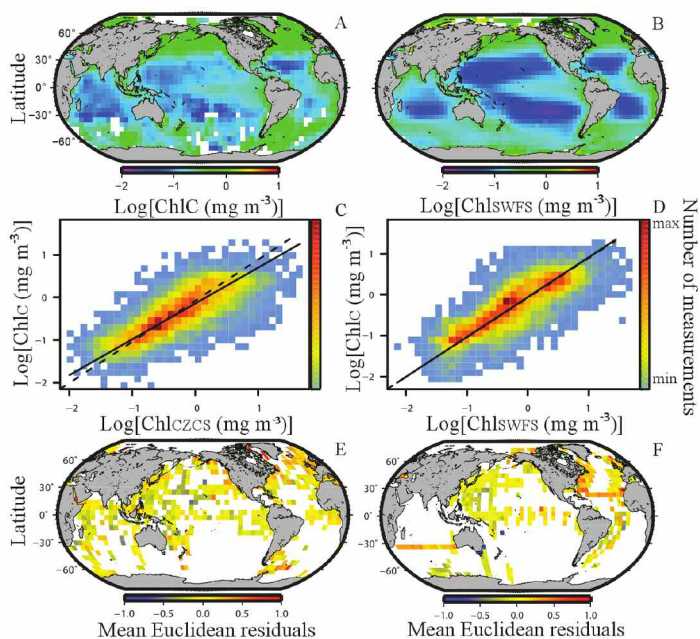


**Fig. 6.** Comparison with satellite data. Mean Chl concentration from (A)  $Chl_C$  and (B)  $Chl_{SWFS}$  per  $5^\circ$  cell. Chl was derived using B-spline interpolation; white indicates lack of data. Relationships between  $Chl_C$  and (C)  $Chl_{CZCS}$ , and (D)  $Chl_{SWFS}$ . Idealized relationships are plotted as dashed lines and fitted RMA regressions are shown as solid lines. Colors depict the number of data per pixel. (E-F) Spatial patterns of the average mean Euclidean residuals from regression fits of  $Chl_C$  and (E)  $Chl_{CZCS}$ , and (F)  $Chl_{SWFS}$  per  $5^\circ$  cell.

imate linear scaling (intercept = 0.01, slope = 0.97,  $r^2 = 0.65$ ; Fig. 6D; Table 2). Interestingly, eliminating  $Chl_{FU}$  from the database led to improved correspondence between  $Chl_C$  and  $Chl_{CZCS}$  ( $r = 0.77$ ; intercept = -0.14; slope = 0.86), and  $Chl_{SWFS}$  ( $r = 0.82$ ; intercept = -0.07; slope = 1). Due to the large number of matchups, all correlation coefficients were statistically significant.

Spatial examination of the standardized Euclidean residuals from the RMA regressions indicated that there was a greater discrepancy between  $Chl_C$  and  $Chl_{SWFS}$  or  $Chl_{CZCS}$  in more coastal areas where Chl concentrations are on average greater and more variable (Fig. 6E & 6F). Spatially explicit models fitted to the residuals confirmed that residuals were, on average, larger in areas closer to coastlines, at higher latitudes, and where Chl values are greater. Since latitude, distance from the nearest coast, and Chl are collinear, univariate models were also fitted to the residuals. The strongest single explanatory variable to explain the residual variation in  $Chl_C$  relative to  $Chl_{CZCS}$  or  $Chl_{SWFS}$  was the average Chl concentration ( $Chl_{SWFS}$ :  $r^2 = 0.05$ ;  $P < 0.0001$  and  $Chl_{CZCS}$ :  $r^2 = 0.16$ ;  $P < 0.0001$ ; Fig. 7). For both matchups, the magnitude of the residuals was insensitive to the average concentration of colored dissolved organic matter (CDOM) in the water, or to changes in the year of sampling. The relationship between  $Chl_C$  and  $Chl_{SWFS}$  or  $Chl_{CZCS}$  was found to be insensitive to the number of measurements used. The strength of the relationships was largely insensitive to reduced sample size, and to the bathymetry, ocean basin, month, or decade when the measurements were collected.

The reliability of the  $Chl_C$  database rests on the assumption that the function used to predict Chl is insensitive to the time and location of sampling and that the error associated with that relationship is random. We were fortunate that the large temporal and spatial overlap between available matchups allowed for a robust test of these assumptions; however, matchups were not available for all times and locations. Although matchups of  $Chl_I$  with water transparency or color were unavailable prior to 1950, the strong correlation and approximately linear scaling between log-transformed  $Chl_I$  and  $Chl_F$  matchups since 1890 confirmed the efficacy of the algorithms used to calibrate them (Table 2). Additionally, the methods used here require accurate measurements of  $Chl_I$  to calibrate  $Chl_T$  and  $Chl_F$ .  $Chl_I$  measurements derived from high

**Table 2.** Regression results of model II RMA models fitted to the Chl matchups from different observational platforms. Estimated regression coefficients, error estimates, bias estimates, coefficient of determination, correlation coefficient, number of matchups, and the temporal and latitudinal span of the available matchups are given.

Comparison	$b1$	$b1$ SE	$b1_{BIAS}$	$b0$	$r^2$	$r$	$r$ raw	$n$	Yr. span	Lat. span
$Chl_I/Chl_T$	1.00	0.01	0.00	0.01	0.65	0.81	0.63	12841	51	154
$Chl_{CZCS}/Chl_T$	0.84	0.02	0.00	-0.13	0.57	0.76	0.49	4376	8	141
$Chl_{SWFS}/Chl_T$	0.97	0.03	0.00	0.04	0.69	0.83	0.58	2244	10	84
$Chl_F/Chl_I$	1.00	0.03	-0.01	0.00	0.47	0.69	0.59	6943	46	146
$Chl_{CZCS}/Chl_F$	0.99	0.05	-0.04	-0.14	0.35	0.59	0.30	3057	8	121
$Chl_{SWFS}/Chl_F$	0.92	0.03	-0.02	0.13	0.68	0.82	0.66	1643	10	54
$Chl_{CZCS}/Chl_I$	0.94	0.02	0.00	-0.13	0.60	0.77	0.43	5805	8	145
$Chl_{SWFS}/Chl_I$	1.01	0.02	0.00	-0.09	0.66	0.81	0.50	9198	12	153
$Chl_F/Chl_T$	1.07	0.01	0.00	-0.02	0.48	0.70	0.53	46180	117	156
$Chl_{CZCS}/Chl_C$	0.84	0.01	-0.01	-0.15	0.58	0.76	0.44	9717	8	148
$Chl_{SWFS}/Chl_C$	0.97	0.01	0.00	-0.06	0.65	0.81	0.51	10204	12	160

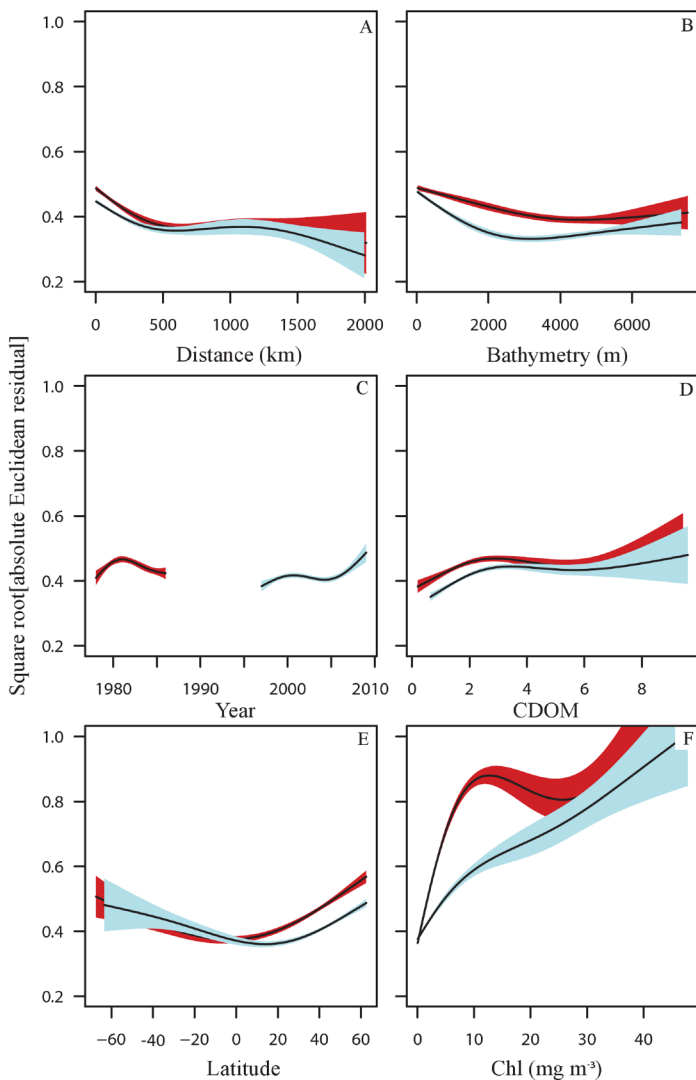


**Fig. 7.** Variability in absolute Euclidean residuals. GAM estimates of the square root-transformed absolute Euclidean residuals from linear RMA models of  $Chl_C$  versus  $Chl_{SWFS}$  (red) and  $Chl_{CZCS}$  (blue) as a function of (A) distance from the nearest coastline; (B) bathymetry; (C) year; (D) colored dissolved organic material (CDOM); (E) latitude; and (F) mean  $Chl$ . The estimated trends are plotted as solid lines and shaded areas represent the 95% Bayesian credible limits for the trends.

performance liquid chromatography (HPLC) are generally regarded as the best performing *in situ* technique, but are not readily available over long time scales. To generate a large enough database of historical measurements,  $Chl_I$  values derived from several *in situ* instruments were used here. Although some methods have been found to underestimate  $Chl$ , relative to HPLC techniques, this error is believed to be small (Trees et al. 1985), with the main source of  $Chl_I$  variability resulting from methodological differences among investigators (Welschmeyer 1994). Although systematic quality control techniques were used to remove measurements associated with these sources of variability, some erroneous

$Chl_I$  measurements may persist and contribute to the unexplained variation in the data.

To enable comparison of the various shipboard and remote sensing methods, the analysis was restricted to the surface layer (upper 20 meters). The  $Chl_C$  data, therefore, may not reflect the integrated chlorophyll values, since the  $Chl$  maximum occurs much deeper in some low-latitude ocean regions (Cullen 1982). Additionally,  $Chl_I$  measurements below 20 m are usually derived from CTD profiles of *in vivo* fluorescence, and variability in the chlorophyll-to-phytoplankton biomass (organic carbon) relationship at these depths is known to produce more uncertain abundance estimates. The use of  $Chl_I$  measurements in the upper 20 m of the water column to infer phytoplankton biomass is a common practice (Behrenfeld et al. 2006; Falkowski and Wilson 1992; Martinez et al. 2009), but it is possible that changes in major oceanographic features such as the mixed layer depth (MLD) may cause corresponding vertical shifts in phytoplankton to waters deeper than 20 m (Saba et al. 2010). If such shifts were occurring, this could cause underestimates of phytoplankton in some ocean regions and would provide a strong incentive for *in situ* observational platforms to expand the vertical sampling range.

### Discussion

Here, we have demonstrated that shipboard measurements of upper ocean water transparency and color can be integrated to derive accurate  $Chl$  fields at global scales, and extending 120 years into the past. Following careful calibration, measurements of  $Chl$  derived from different observational platforms have been combined into a single publicly available database (see web appendices). This study was conducted using similar approaches to those developed in a previous study (Boyce et al. 2010), but incorporating additional data and several suggested improvements (Boyce et al. 2011; Mackas 2011; McQuatters-Gollop et al. 2011; Rykaczewski and Dunne 2011). First, the calibrated database presented here was generated from a larger and more comprehensive set of measurements, and includes the FU-derived  $Chl$  measurements not previously used. Consequently, our calibrated  $Chl$  database is more spatially and temporally complete, and contains an additional 199,679 measurements. Unfortunately, we could not include plankton color measurements from the continuous plankton recorder (CPR) dataset (see Reid et al. 2003) in our analysis. Our goal was to produce a publicly available database of  $Chl$  measurements, and as the raw CPR data are proprietary, we were unable to include them here. Furthermore, the size of the CPR silk (>250  $\mu m$ ) is designed to sample large zooplankton, and may not quantitatively sample smaller size fractions of the phytoplankton.

Second, several improvements have been made to the statistical methods used to identify implausible  $Chl$  measurements. Such improvements include, for instance, the treatment of zero  $Chl_I$  measurements, the identification of erroneous CTD-derived  $Chl_I$  measurements, and the use of

spatial filters. Last, the Chl measurements presented here were directly calibrated from a database of independent, quality verified *in situ* Chl measurements, rather than from a previously established algorithm. Further, the calibration algorithms were developed using an unprecedented number of quality controlled *in situ* Chl measurements ( $n = 12,841$  Secchi matchups;  $n = 6943$  Forel-Ule matchups); this represents a considerable improvement over the number of matchups typically used to calibrate chlorophyll fields from remotely sensed water-leaving radiances ( $n = 60$  CZCS matchups;  $n = 2853$  SWFS matchups) (Evans and Gordon 1994; O'Reilly et al. 2000). This increases confidence in our approach and allows for a robust verification of the statistical assumptions of the calibration and validation methods.

The database of calibrated chlorophyll measurements presented here remains undersampled, as there are still some large data gaps, particularly in the Southern hemisphere. Despite this, we believe that the available data can and should be used to explore trends in global or regional phytoplankton dynamics before the satellite era (1979–86, 1997–2010). The separation of yearly-to-decadal fluctuations from longer-term phytoplankton dynamics is a frequently acknowledged challenge (Behrenfeld et al. 2006; Henson et al. 2010; Martinez et al. 2009), and is directly related to the scarcity of calibrated phytoplankton abundance measurements in the pre-satellite era (<1978). This lack of an adequate dataset may be partially responsible for the large variability in estimated trends in regional or global phytoplankton concentrations or primary production (Antoine et al. 2005; Behrenfeld et al. 2006; Falkowski and Wilson 1992; Gregg et al. 2005; Gregg and Conkright 2002; Gregg et al. 2003; Venrick et al. 1987). Accordingly, the calibrated global phytoplankton time series presented here may enable the assessment of ocean biological variability over a range of time and spatial scales and help in establishing the 'missing baseline' (Pauly 1995) against which to compare contemporary trends and estimates. Given the broad importance of phytoplankton to global marine ecosystems and processes (Behrenfeld 2011; Falkowski 2012), the potential applications of the calibrated phytoplankton time-series are considerable. To facilitate optimal use of the described dataset, we make it available as a web appendix to this paper. The data set is presented as a user-friendly text file that can be easily imported into most software platforms or in a spreadsheet. The associated metadata is also contained in the header of this file and includes a description of the variables included in the data set, the units they are measured in, the relevant citation for the data set, and contact information if users have any relevant questions.

### Comments and recommendations

For those seeking to analyze these data, several attributes must be considered. First, to accurately calibrate Secchi and Forel-Ule measurements, we eliminated all measurements close to coastlines, all *in situ* Chl measurements below a depth

of 20 m, all Secchi measurements less than 6 m, and all Forel-Ule measurements with a color value of less than 2 and greater than 10. Although this was necessary to ensure the accuracy of calibration algorithms, the resulting database should not be considered to represent a complete phytoplankton inventory. Second, since the calibrated Chl values were derived from deterministic models, they contain no measurement error and are thus considered non-random. Alternately, the *in situ* Chl measurements were not derived from a model; thus, they contain measurement error and are considered random. Hence the calibrated values will, on average, contain the same mean as the *in situ* measurements but will have a lower variance. Last, spatial and temporal matchups between Chl measurements derived from different sensors, and observational platforms are necessary for calibration and validation, but may violate the assumption of independence required by many statistical analyses.

### References

- Acker, J. G., and G. Leptoukh. 2007. Online analysis enhances use of NASA earth science data. *Trans. AGU* 88:14-17 [doi:10.1029/2007EO020003].
- Akima, H. 1978. A method of bivariate interpolation and smooth surface fitting for irregularly distributed data points. *ACM Trans. Math. Software* 4:148-159 [doi:10.1145/355780.355786].
- Antoine, D., A. Morel, H. R. Gordon, V. F. Banzon, and R. H. Evans. 2005. Bridging ocean color observations of the 1980s and 2000s in search of long-term trends. *J. Geophys. Res.* 110:1-22 [doi:10.1029/2004JC002620].
- Augustin, N. H., M. A. Muggleston, and S. T. Buckland. 1996. An autologistic model for the spatial distribution of wildlife. *J. Appl. Ecol.* 33:339-347 [doi:10.2307/2404755].
- Behrenfeld, M. 2011. Uncertain future for ocean algae. *Nature Climate Change* 1:33-34 [doi:10.1038/nclimate1069].
- Behrenfeld, M. J., and others. 2006. Climate-driven trends in contemporary ocean productivity. *Nature* 444:752-755 [doi:10.1038/nature05317].
- Boyce, D. G., M. R. Lewis, and B. Worm. 2010. Global phytoplankton decline over the past century. *Nature* 466:591-596 [doi:10.1038/nature09268].
- , ———, and ———. 2011. Boyce et al. reply. *Nature: Brief communications* arising 472:E8-E9.
- Boyer, T. P., and others. 2009. World ocean database 2009, p. 217. *In* S. Levitus [ed.], NOAA Atlas NESDIS 66. National Oceanographic Data Center Ocean Climate Center.
- Charlson, R. J., J. E. Lowelock, M. O. Andreae, and S. G. Warren. 1987. Oceanic phytoplankton, atmospheric sulphur, cloud albedo and climate. *Nature* 326:655-661 [doi:10.1038/326655a0].
- Chassot, E., F. Melin, O. Le Pape, and D. Gascuel. 2007. Bottom-up control regulates fisheries production at the scale of eco-regions in European seas. *Mar. Ecol. Prog. Ser.* 343:45-55 [doi:10.3354/meps06919].

- , and others. 2010. Global marine primary production constrains fisheries catches. *Ecol. Lett.* 13:495-505 [doi:10.1111/j.1461-0248.2010.01443.x].
- Collier, A., G. M. Finlayson, and E. W. Cake. 1968. On the transparency of the sea. *Limnol. Oceanogr.* 13:391-394 [doi:10.4319/lm.1968.13.2.0391].
- Conkright, M. E., and others. 2002. World ocean atlas 2001: Objective analyses, data statistics, and Fig.s, p. 17. CD-ROM Documentation.
- Cullen, J. 1982. The deep chlorophyll maximum: comparing vertical profiles of chlorophyll a. *Can. J. Fish. Aquat. Sci.* 39:791-801 [doi:10.1139/f82-108].
- Doney, S. C., D. M. Glover, S. J. McCue, and M. Fuentes. 2003. Mesoscale variability of Sea-viewing Wide Field-of-view Sensor (SeaWiFS) satellite ocean color: Global patterns and spatial scales. *J. Geophys. Res. Oceans* 108:1-19.
- Dormann, C. F., and others. 2007. Methods to account for spatial autocorrelation in the analysis of species distributional data: a review. *Ecography* 30:609-628 [doi:10.1111/j.2007.0906-7590.05171.x].
- Evans, E. H., and H. R. Gordon. 1994. Coastal zone color scanner 'system calibration': A retrospective examination. *J. Geophys. Res.* 99:7293-7307 [doi:10.1029/93JC02151].
- Falkowski, P. 2012. The power of plankton. *Nature* 483:S17-S20 [doi:10.1038/483S17a].
- , and C. Wilson. 1992. Phytoplankton productivity in the North Pacific ocean since 1900 and implications for absorption of anthropogenic CO<sub>2</sub>. *Nature* 358:741-743 [doi:10.1038/358741a0].
- Forel, F. A. 1890. Une nouvelle forme de la gamme de couleur pour l'étude de l'eau des lacs. *Archives des sciences physiques et naturelles/Societe de physique et d'histoire naturelle de geneve* 6.
- Geider, R. J. 1987. Light and temperature-dependence of the carbon to chlorophyll-a ratio in microalgae and cyanobacteria - implications for physiology and growth of phytoplankton. *New Phytol.* 106:1-34 [doi:10.1111/j.1469-8137.1987.tb04788.x].
- Gregg, W. W., and M. E. Conkright. 2001. Global seasonal climatologies of ocean chlorophyll: Blending in situ and satellite data for the Coastal Zone Color Scanner era. *J. Geophys. Res.* 106:2499-2515 [doi:10.1029/1999JC000028].
- , and ———. 2002. Decadal changes in global ocean chlorophyll. *Geophys. Res. Lett.* 29:1730-1734 [doi:10.1029/2002GL014689].
- , M. E. Conkright, P. Ginoux, J. E. O'Reilly, and N. W. Casey. 2003. Ocean primary production and climate: Global decadal changes. *Geophys. Res. Lett.* 30:1909-1813 [doi:10.1029/2003GL016889].
- , N. W. Casey, and C. R. McClain. 2005. Recent trends in global ocean chlorophyll. *Geophys. Res. Lett.* 32:1-5 [doi:10.1029/2004GL021808].
- Gumpertz, M. L., J. M. Graham, and J. B. Ristaino. 1997. Autologistic model of spatial pattern of phytophthora epidemic in bell pepper: effects of soil variables on disease presence. *J. Agric. Biol. Envir. Stat.* 2:131-156 [doi:10.2307/1400400].
- Hastie, T., and R. Tibshirani. 1986. Generalized additive models. *Statist. Sci.* 1:297-318 [doi:10.1214/ss/1177013604].
- Henson, S. A., and others. 2010. Detection of anthropogenic climate change in satellite records of ocean chlorophyll and productivity. *Biogeosciences* 7:621-640 [doi:10.5194/bg-7-621-2010].
- Hovis, W. A., and others. 1980. Nimbus-7 coastal zone color scanner: system description and initial imagery. *Science* 210:60-63 [doi:10.1126/science.210.4465.60].
- Huot, Y., M. Babin, F. Bruyant, C. Grob, M. S. Twardowski, and H. Claustre. 2007. Does chlorophyll a provide the best index of phytoplankton biomass for primary productivity studies? *Biogeosci. Discuss.* 4:707-745 [doi:10.5194/bgd-4-707-2007].
- International Ocean-Colour Coordinating Group [I.O.C.C.G.] 2007. Ocean-colour data merging. *In* W. Gregg [ed.], Reports of the International Ocean-Colour Coordinating Group. IOCCG Report Nr 6. <<http://www.ioccg.org/reports/report6.pdf>>
- Jeffrey, S. W., R. F. C. Mantoura, and S. W. Wright. 1997. Phytoplankton pigments in oceanography. UNESCO.
- Legendre, P., and L. Legendre. 1998. Numerical ecology, 2nd ed. Elsevier Science.
- Levy, G., and R. A. Brown. 1986. A simple objective analysis scheme for scatterometer data. *J. Geophys. Res.* 91:5153-5158 [doi:10.1029/JC091iC04p05153].
- Lewis, M. R., N. Kuring, and C. Yentsch. 1988. Global patterns of ocean transparency: implications for the new production of the open ocean. *J. Geophys. Res.* 93:6847-6856 [doi:10.1029/JC093iC06p06847].
- Lorenzen, C. L. 1966. A method for the continuous measurement of in vivo chlorophyll concentration. *Deep Sea Res.* 13:223-227.
- Mackas, D. L. 2011. Does blending of chlorophyll data bias temporal trend? *Nature: Brief communications arising* 472:E4-E5.
- Mahadevan, A., and J. W. Campbell. 2002. Biogeochemical patchiness at the sea surface. *Geophys. Res. Lett.* 29:31-32.
- Mantoura, R. F. C., and C. A. Llewellyn. 1983. The rapid determination of algal chlorophyll and carotenoid pigments and their breakdown products in natural waters by reverse-phase high-performance liquid chromatography. *Anal. Chim. Acta* 151:297-314 [doi:10.1016/S0003-2670(00)80092-6].
- Martinez, E., D. Antoine, F. D'Ortenzio, and B. Gentili. 2009. Climate-driven basin-scale decadal oscillations of oceanic phytoplankton. *Science* 326:1253-1256 [doi:10.1126/science.1177012].
- McClain, C. R., G. C. Feldman, and S. B. Hooker. 2004. An overview of the SeaWiFS project and strategies for producing a climate research quality global ocean bio-optical time series. *Deep-Sea Res. II* 51:5-42 [doi:10.1016/j.dsr2.2003.11.001].

- McQuatters-Gollop, A., and others. 2011. Is there a decline in marine phytoplankton? *Nature: Brief communications arising* 472:E6-E7.
- Morel, A., and B. Gentili. 2009. A simple band ratio technique to quantify the colored dissolved and detrital organic material from ocean color remotely sensed data. *Rem. Sens. Environ.* 113:998-1011 [doi:10.1016/j.rse.2009.01.008].
- Murtugudde, R., R. J. Beauchamp, C. R. McClain, M. R. Lewis, and A. Busalacchi. 2002. Effects of penetrative radiation on the upper tropical ocean circulation. *J. Clim.* 15:470-486 [doi:10.1175/1520-0442(2002)015<0470:EOPROT>2.0.CO;2].
- O'Reilly, J. E., and others. 2000. Ocean color chlorophyll a algorithms for SeaWiFS, OC2, and OC4: Version 4, p. 9-23. *In* S. B. Hooker and E. R. Firestone [eds.], *SeaWiFS Post-launch Technical Report Series*, Vol. 11. NASA, Goddard Space Flight Center.
- Pauly, D. 1995. Anecdotes and the shifting baseline syndrome of fisheries. *Trends Ecol. Evol.* 10:430 [doi:10.1016/S0169-5347(00)89171-5].
- Preisendorfer, R. W. 1986. Secchi disk science: Visual optics of natural waters. *Limnol. Oceanogr.* 31:909-926 [doi:10.4319/lo.1986.31.5.0909].
- Raitos, D. E., P. C. Reid, S. J. Lavender, M. Edwards, and A. J. Richardson. 2005. Extending the SeaWiFS chlorophyll data set back 50 years in the northeast Atlantic. *Geophys. Res. Lett.* 32:1-4 [doi:10.1029/2005GL022484].
- Reid, P. C., J. M. Colebrook, J. B. L. Matthews, and J. Aiken. 2003. Continuous Plankton Recorder Team, the Continuous Plankton Recorder: concepts and history, from Plankton Indicator to undulating recorders. *Prog. Oceanogr.* 58:117-173 [doi:10.1016/j.pocean.2003.08.002].
- Ripley, B. D., and M. Thompson. 1987. Regression techniques for the detection of analytical bias. *Analyst* 112:377-383 [doi:10.1039/an9871200377].
- Roemmich, D., and J. McGowan. 1995. Climatic warming and the decline of zooplankton in the California current. *Science* 267:1324-1326 [doi:10.1126/science.267.5202.1324].
- Rybczewski, R., and J. P. Dunne. 2011. A measured look at ocean chlorophyll trends. *Nature: Brief communications arising* 472:E5-E6.
- Saba, V., and others. 2010. Challenges of modeling depth-integrated marine primary productivity over multiple decades: A case study at BATS and HOTS. *Global Biogeochem. Cycles* 24:1-21 [doi:10.1029/2009GB003655].
- Sabine, C. L., and others. 2004. The oceanic sink for anthropogenic CO<sub>2</sub>. *Science* 305:367-371 [doi:10.1126/science.1097403].
- Siegel, D. A., S. Maritorena, N. B. Nelson, and M. J. Behrenfeld. 2005. Independence and interdependence of global ocean color properties; Reassessing the bio-optical assumption. *J. Geophys. Res.* 110: C07011 [doi:10.1029/2004JC002527].
- Sokal, R. R., and F. J. Rohlf. 1995. *Biometry—The principles and practice of statistics in biological research*. W.H. Freeman.
- Stokes, G. G. 1864. On the supposed identity of biliverdin with chlorophyll with remarks on the constitution of chlorophyll. *Proc. Roy. Soc.* 13:144-145.
- Trees, C. C., M. C. I. Kennicutt, and J. Brooks. 1985. Errors associated with the standard fluorometric determination of chlorophylls and phaeopigments. *Mar. Chem.* 17:1-12 [doi:10.1016/0304-4203(85)90032-5].
- Tyler, J. E. 1968. The Secchi disk. *Limnol. Oceanogr.* 13:1-6 [doi:10.4319/lo.1968.13.1.0001].
- Venrick, E. L., J. A. McGowan, D. R. Cayan, and T. L. Hayward. 1987. Climate and chlorophyll a: a long-term trends in the Central North Pacific Ocean. *Science* 238:70-72 [doi:10.1126/science.238.4823.70].
- Welschmeyer, N. A. 1994. Fluorometric analysis of chlorophyll a in the presence of chlorophyll b and phaeopigments. *Limnol. Oceanogr.* 39:1985-1992 [doi:10.4319/lo.1994.39.8.1985].
- Wernand, M. R., and H. J. van der Woerd. 2010. Ocean colour changes in the North Pacific since 1930. *J. Eur. Opt. Soc.* 5:1-6 [doi:10.2971/jeos.2010.10015s].
- Wiltshire, K. H., S. Harsdorf, B. Smidt, G. Blocker, R. Reuter, and F. Schroeder. 1998. The determination of algal biomass (as chlorophyll) in suspended matter from the Elbe estuary and the German Bight: A comparison of high-performance liquid chromatography, delayed fluorescence and prompt fluorescence methods. *J. Exp. Mar. Biol. Ecol.* 222:113-131 [doi:10.1016/S0022-0981(97)00141-X].
- Wood, S. 2006. *Generalized additive models: an introduction with R*. Chapman & Hall/CRC.
- Yentsch, C. S., and D. W. Menzel. 1963. A method for the determination of phytoplankton chlorophyll and phaeophytin by fluorescence. *Deep Sea Res.* 10:221-231.

Submitted 8 February 2012

Revised 15 June 2012

Accepted 19 June 2012